



ISSN: 0976-3031

Available Online at <http://www.recentscientific.com>

CODEN: IJRSFP (USA)

International Journal of Recent Scientific Research
Vol. 8, Issue, 6, pp. 17640-17645, June, 2017

**International Journal of
Recent Scientific
Research**

DOI: 10.24327/IJRSR

Research Article

FACILE SYNTHESIS OF N-ZnO NANOSTRUCTURES BY THERMAL DECOMPOSITION OF SCHIFF BASE ZINC COMPLEX PRECURSOR: STRUCTURAL, OPTICAL, ANTIMICROBIAL AND PHOTOCATALYTIC PROPERTIES

Remya Simon¹, Manigandan Ramadoss², Narayanan vengidusamy²,
Nisha George¹ and Mary N.L^{1*}

¹Department of Chemistry, Stella Maris College, Chennai 600 08, Tamil Nadu, India

²Department of Inorganic Chemistry, University of Madras, Chennai, Tamil Nadu, India

DOI: <http://dx.doi.org/10.24327/ijrsr.2017.0806.0396>

ARTICLE INFO

Article History:

Received 16th March, 2017
Received in revised form 25th
April, 2017
Accepted 23rd May, 2017
Published online 28th June, 2017

Key Words:

Schiff base Zinc complexes, N-ZnO,
Photocatalytic activity, band gap, Pore size.

ABSTRACT

Zn (II) complex was synthesized by using Schiff base terephthalaldehyde-o-phenylenediamine as Schiff base ligand and characterized by FTIR spectroscopic methods. N-ZnO (nitrogen-rich zinc oxide) nanoparticles were prepared by calcination of Schiff base zinc complex at 500 °C. The average grain size and structural parameters were analyzed using X-ray diffraction studies. The X-ray diffraction analysis of the sample showed the formation of nanoparticles with hexagonal ZnO structure. Size of the particles and presence of doped nitrogen in the zinc oxide nanostructures were examined by HR-SEM-EDX. Furthermore, the optical properties like band gap, absorbance measurement of zinc oxide were extensively examined. The surface area and pore size of ZnO were characterized. In addition, a clear relationship between the porous nature and photocatalytic characteristics of N-rich ZnO was observed. The photocatalytic degradation property of N-rich ZnO nanoparticles were examined with methylene blue under the visible light irradiation. Overall, N-rich ZnO nanoparticles exhibited superior photocatalytic behavior compared to commercial available ZnO nanoparticles.

Copyright © Remya Simon *et al*, 2017, this is an open-access article distributed under the terms of the Creative Commons Attribution License, which permits unrestricted use, distribution and reproduction in any medium, provided the original work is properly cited.

INTRODUCTION

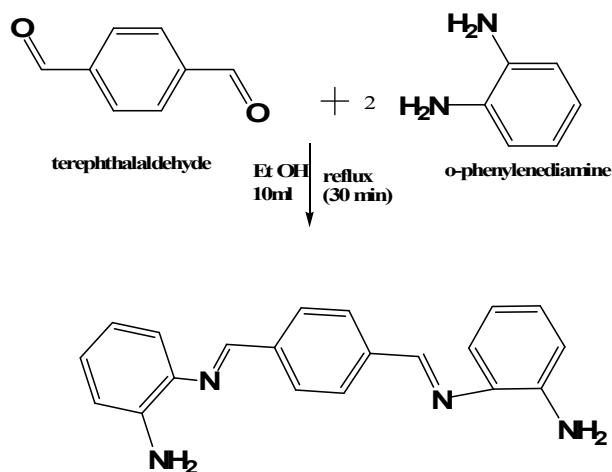
Metal oxide nanomaterials have, in the last few years, been of boundless interest among researchers who have studied its significance in the fields of technology and scientific application [1]. In photocatalysis, the activity is dependent on the catalyst's ability to generate/produce electron-hole pairs to undergo redox reactions. Bottom-up approached synthesis of ZnO has concerned attention in the semiconductor photocatalysis of nanomaterials due to its flexibility in morphology and its unique physicochemical properties with a wide band-gap in the ultraviolet region at approximately 3.2-3.4 eV [2-4]. The application of such materials in memory devices, photocatalysis and gas sensing are due to its unique magnetic, electrical, electronic, absorption and emission properties. Furthermore, the behavior of nanostructured metal oxides completely depends on the small grain sizes of nanoparticles [5-7]. The unique chemical and optical features of ZnO, such as photosensitivity, low cost and biological inertness, which induce interest in investigation in photocatalytic applications, good chemical/physical stability,

and low toxicity [8, 9]. In addition, size modification in the structural, optical and electronic properties of doped ZnO nanomaterials has been widely reported [10]. Porous nanostructures with nanoscale are suitable materials because their special structures provide a large surface-to-volume ratio that can enhance the physicochemical properties of the semiconductors. Zinc oxide was synthesized as nanostructured material with the assistance of surfactants or polymers [11-13]. The optical, and photocatalytic property of size-reduced nanophase obtained by single precursor (zinc Schiff's bases) and facile synthesis in the absence of any polymer, capping agents or surfactants is the focus of the present investigation. Schiff's bases resulting from amines and aromatic aldehydes and their complexes have an extensive diversity of applications in chemical and biological sciences. [14-16]. This method has potential advantages, including high yield of products thus exempting the need for special equipment, easy to prepare and more stable because of the chelate formation [17]. In this paper, nitrogen-rich ZnOs derived from Schiff base metal complexes of terephthalaldehyde-o-phenylenediamine zinc complex. We used the thermal decomposition method for the preparation of

*Corresponding author: **Mary N.L**

Department of Chemistry, Stella Maris College, Chennai 600 08, Tamil Nadu, India

N-rich ZnO nanoparticles from Schiff base complexes of terephthalaldehyde-o-phenylenediamine zinc nitrate complex. Porous N-rich ZnO nanostructures with a relatively regular morphology, crystallinity, size, specific surface area, defects and surface properties of zinc oxide nanostructures were evaluated carefully.



Scheme 1 Mechanism of synthesis of N,N'-bis(1,2-phenylenediamide)-terephthalaldehyde Schiff base ligand.

Experimental

Materials

Terephthalaldehyde, o-phenylenediamine, zinc nitrate, ethanol, tetrahydrofuran, sodium acetate, and methylene blue are purchased from Sigma Aldrich, SD Fine Chemicals and Merck Specialties Private Limited.

Synthesis of Schiff base from terephthalaldehyde and o-phenylenediamine

1.08 g of terephthalaldehyde (1 M) was mixed with 20 ml of ethanol taken in a round bottomed flask. To this, 2.68 g o-phenylenediamine (2 M) was added and refluxed for 30 min on a water bath and cooled. An orange colour solid precipitate of N,N'-bis(1,2-phenylenediamide)-terephthalaldehyde Schiff base was obtained. The precipitate obtained was filtered and dried.

Synthesis of zinc complex from N,N'-bis(1,2-phenylenediamide)-terephthalaldehyde ligand

2.24g of N,N'-bis(1,2-phenylenediamide)-terephthalaldehyde ligand(o-PTA) was dissolved in 10ml of tetrahydrofuran taken in a RB flask. To this zinc nitrate was added and refluxed for one hour on a water bath. 0.01 g of sodium acetate was added to maintain the pH and heating was continued for 30 min and cooled. A solid precipitate of zinc complex was obtained. The precipitate obtained was filtered and washed thoroughly with THF.

Synthesis of N-rich ZnO

Prepared zinc complexes were taken in a pre-heated silica crucible kept in a muffle furnace for 3 h at 500 °C and cooled. Thermal decomposition of zinc complexes were converted into corresponding zinc oxide nanoparticles.

Antibacterial studies

The antimicrobial activity of prepared N-rich ZnO nanoparticles was carried out by agar well diffusion method. The wells were punched over the agar plates and 100 µg of N-rich ZnO nanoparticles obtained by the thermal decomposition of Schiff base zinc complex from chemical synthesis were dispersed in DMSO was placed in the well. The plates were incubated for 24 h at 37 °C. After incubation the diameter of inhibitory zones formed around each disc were measured in mm and recorded.

Measurement of photocatalytic activity

The photocatalytic activity of N-rich ZnO nanoparticles was achieved using catalytic reactor, which contains 100 ml of methylene blue solution, and 25 mg of catalyst. Visible light irradiation was carried out with the assistance of halogen lamps. The same experimental condition followed for all the reactions. Samples (3 ml) were collected during 15 min interval of irradiation.

Characterization methods

FTIR spectra of samples were recorded on a Nicolet spectrometer using KBr pellets. X-ray diffraction (XRD) analysis was measured on a Rich Siefert 3000 diffractometer. High resolution scanning electron microscopy analysis was done by FEI Quanta FEG 200 High Resolution Scanning Electron Microscope (HRSEM). BEL SORP mini II analyzer was used to measure the N₂ adsorption-desorption isotherms at liquid N₂ temperature. The samples were degassed at 300 °C for 6 h. Surface area, pore volume and pore size distributions was calculated by the BET method, nitrogen adsorption, and desorption isotherms, respectively, with the help of Barrett Joyner Halenda (BJH) method. The photocatalytic activity was measured using a double beam UV-Vis spectrophotometer (Shimadzu UV-1700).

RESULT AND DISCUSSION

The functional group analysis of the prepared o-PTA, zinc complex and calcined ZnO were characterized using FT-IR spectroscopy, which was shown in Fig. 1 respectively. In Fig. 1a, the spectrum shows that the very strong and broad band observed at 3350 cm⁻¹ was due to the stretching of the O-H groups of the coordinated water. The FTIR spectra of o-PTA shows the appearance of strong bands at 1618 cm⁻¹ which can be attributed to imine group (C=N). The formation of the imine bonds could be happened by the Schiff base condensation of aldehyde and amine groups. The medium band at 1498 cm⁻¹ can be assigned to the aromatic C=C [18]. In the zinc complex, band appears at a frequency lower than that of the free ligand, indicating the formation of metal coordination. Mainly, the ν(C=N) band at 1618 cm⁻¹ shifts to lower frequency (1611) refers to the involvement of the azomethine nitrogen in coordination with zinc (Zn-N). This clearly indicates that the involvement of nitrogen atom in coordination due to reduction in the electron density in the azomethine linkage [19]. Hence, the IR spectrum obtained for zinc complexes concluded that the ligand behaves as a ligand coordinated to the zinc ions via azomethine nitrogen. The FTIR spectrum obtained for the thermally decomposed zinc complex shows few peaks corresponds to the N-rich zinc oxide were given in Fig. 1b. The

strong band at about 492 cm^{-1} was assigned to the stretching vibration of Zn-O bond. The obtained result concludes the presence nitrogen groups in the N-rich ZnO [20].

Table 1

Compounds	γ C=N cm^{-1}	γ O-H cm^{-1}	γ C=C cm^{-1}	γ C-H cm^{-1}
o-PTA	1618	3524	1498	3140
Zn o-PTA	1611	3481	1565	3067

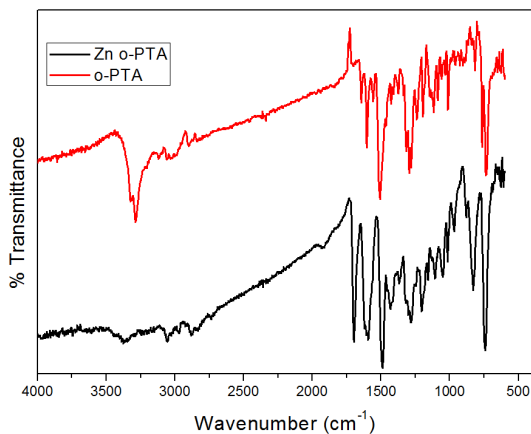


Fig 1a FTIR Spectra of Zn-o-PTA and o-PTA

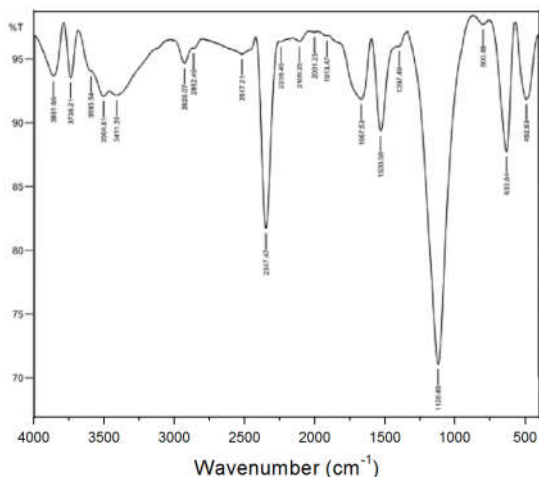


Fig 1b FTIR spectrum of N-rich ZnO

The XRD peaks shown in fig. 2 indicate hexagonal Zincite structure of ZnO. It exhibit 2θ values at 36.19, 31.71, 34.18, 56.47 equivalent to (101), (100), (002), (013) planes respectively. Diffraction patterns are in good agreements with the reported data (JCPDS No. 96-900-4182). The average crystallite size of the samples were calculated using highest intensity diffraction peaks according to Scherrer formula given by the equation

$$D = 0.9\lambda / \beta \cos\theta \quad (1)$$

Where, λ = X-ray wavelength, β = full width half maximum (FWHM), D = average grain size, θ = diffraction angle. The average crystallite size of the N-ZnO was calculated to be 52 nm.

In order to investigate the morphology of the synthesized N-rich ZnO nanoparticles, high resolution scanning electron microscopy (HRSEM-EDAX) images were examined. HRSEM image of N-rich ZnO nanoparticles was shown in Fig. 3(a-c).

The zinc oxide spherical nanostructures obtained by thermal decomposition was found to have average size of 249 nm.

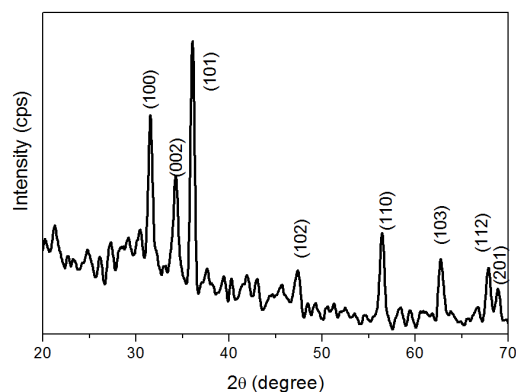


Fig 2 XRD patterns of N-ZnO

The magnification images are given in Fig 3b, show uniform spherical particles with broken surfaces. The elements present in the manganese oxide nanoparticles was confirmed by EDAX analysis which is shown in Fig. 3c. The presence of zinc (Zn), nitrogen (N), carbon (C) and elemental oxygen (O) was identified by this technique. The signals obtained for carbon were observed from the support (carbon tape) of the sample during the measurements which gave carbon signal in the EDAX spectrum. Presence of nitrogen atom in EDAX was in good agreement with the FTIR spectrum, which confirms the N-rich nature of obtained zinc oxide.

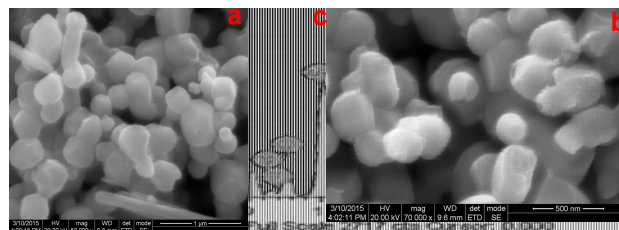


Fig 3 HRSEM-EDAX images of N-rich ZnO NPs

In UV-visible spectroscopy, the basic optical band gap energy or direct allowed transition between valence to conduction band excitation of N-rich ZnO was calculated using Tauc's relation (Fig. 4). Results confirm the presence of semiconducting nature (0-3.5 eV). The nature of the calculated band gap energy value of N-rich ZnO nanoparticles are 3.14 eV. The obtained absorption band with a sharp cut off at 388 nm (Fig. 4) of sample ZnO NPs, is assigned to the phase of ZnO. It does not show any absorbance in the visible region due to the absence of d-d transition. Absorption spectra were carried out using DRS UV-Vis spectrometer, in order to characterize the optical absorbance properties of the ZnO, as presented in Fig. 4. The band gap E can be calculated from Eq. (2) [20, 21]:

$$(\alpha h\nu) = A(h\nu - E_g)^2 \quad (2)$$

Where A = constant, α = is the absorption coefficient, and E_g = band gap and n equals either 1/2 for a direct allowed transition or 2 for an indirect allowed transition. The Tauc plot of $(\alpha h\nu)^2$ vs $h\nu$ have been used to deduce the direct band gaps of obtained sample, which were shown in Fig. 4 (inset). The value of Energy ($E=h\nu$) extrapolated to zeroth value of α gives the basic optical band gap energy of N-rich ZnO was 3.14 eV. The

decrease in the band gap value could be due to the lattice order-disorder nature of N-rich ZnO.

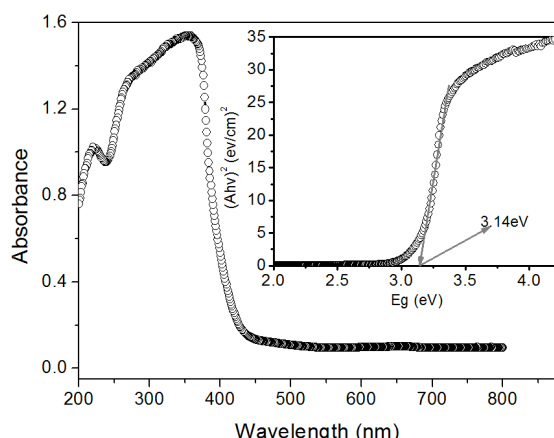


Fig 4 DRS-UV-Vis spectrum [inset: Tauc plot] of N-ZnO

Nitrogen adsorption and desorption properties provide the information on the pore characteristics of N-ZnO nanostructure (Fig. 5). BET surface areas, and pore volumes were measured to be 4.222m²/g and 0.006 cc/g, respectively. The isotherm is type IV classification with type H₁ hysteresis (Fig.5), which is characteristic of adsorption of mesoporous materials. The multimodal micro-pores can be ascribed to the formation of network with different cavities due to the decomposition of Schiff base complex. Laybourn *et al.* reported the one pot polycondensation reactions of terephthalaldehyde and 2, 4-diaminotoluene which has a similar molecular structure with m-phenylenediamine, and resultant sample also shows multimodal micropores [22]. Such high surface area and multimodal pore distributions are responsible for the enhanced photocatalytic degradation of methylene blue.

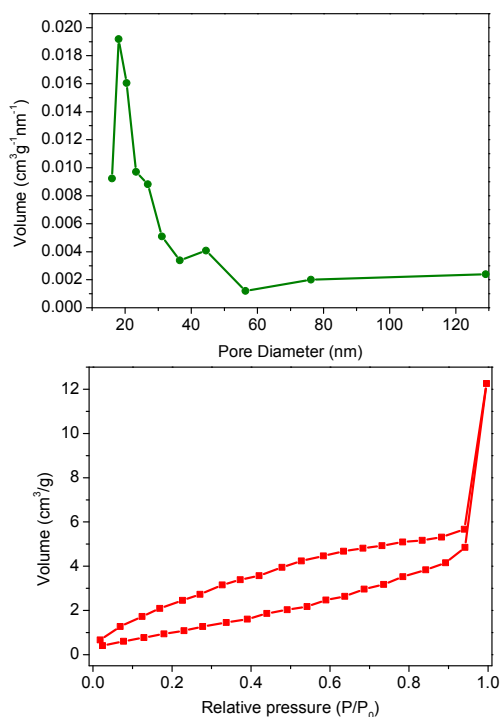


Fig 5 (a) Nitrogen adsorption/desorption isotherms and (b) pore size distribution of N-rich ZnO.

Antibacterial activity of N-rich ZnO nanoparticles

Two gram negative bacteria: Escherichia coli and Klebsiella pneumoniae were used for the study of antibacterial activity. In a comparative study of inhibition values of the nanoparticles between these two negative bacteria, E coli were found to have better activity than the other (Table.1).

Organisms	Zone of Inhibition (mm)	
	ZnO	Negative control (DMSO)
<i>E. coli</i>	12	0
<i>K. pneumoniae</i>	9	0

Photocatalytic degradation of MB

The photocatalytic study of methylene blue was carried out by the presence of semiconducting zinc oxide. The degradation was observed spectrophotometrically (Fig. 6). The photocatalytic activity of N-rich ZnO nanoparticles was observed by degradation of MB with dark, halogen visible lamp, and solar irradiation were compared. The required N-rich ZnO catalyst was mixed with aqueous solution of methylene blue and irradiated by different light source with time interval. From the spectra, it is clearly observed that the concentration of dye decreases with the increasing irradiation time, which is shown by the significant decrease in UV-Visible absorbance at the wavelength of 660 nm. Pure ZnO showed negligible visible-light photocatalytic activity due to the large band gap and the nonexistence of absorption in the visible region. N-rich ZnO nanoparticles synthesized by this simple method showed lower band gap ($E_g=3.14$ eV) compared with the reported results ($E_g > 3.4$ eV) [23]. N-ZnO nanoparticles show significantly high photocatalytic activity in both halogen lamp and solar irradiation by the appreciable decrease in its band gap. The decrease in the band gap value might be due to the increase in the surface defects. The active surface sites and surface defects are mainly attributed by the functionalized nitrogen in the zinc oxide nanostructure. By using the following formula, the percentage (%) of degradation of the methylene blue can be determined.

$$\% \text{ of degradation} = (A_t - A_0 / A_0) * 100$$

where A_0 and A_t are initial and time coursed dye concentrations respectively.

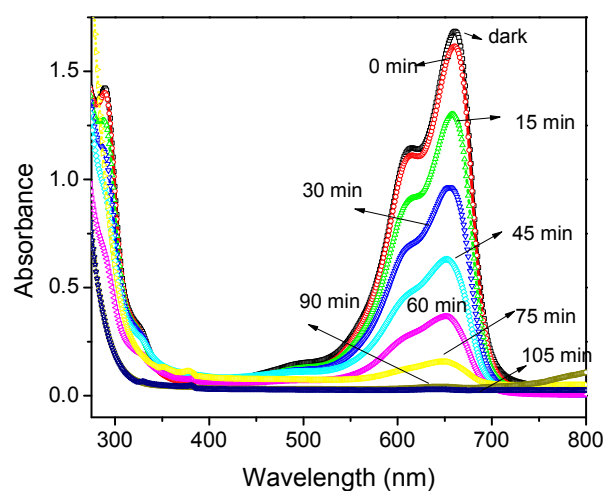


Fig 6 Photodegradation of MB under solar irradiation with different time intervals.

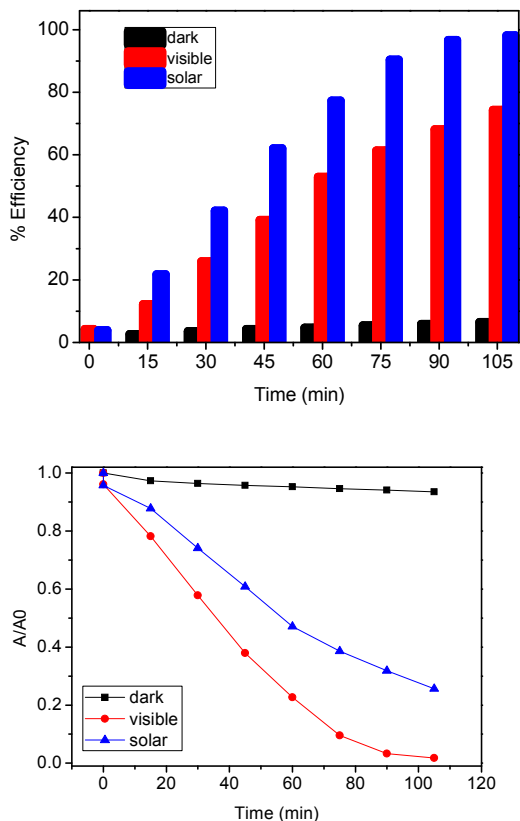
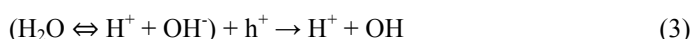
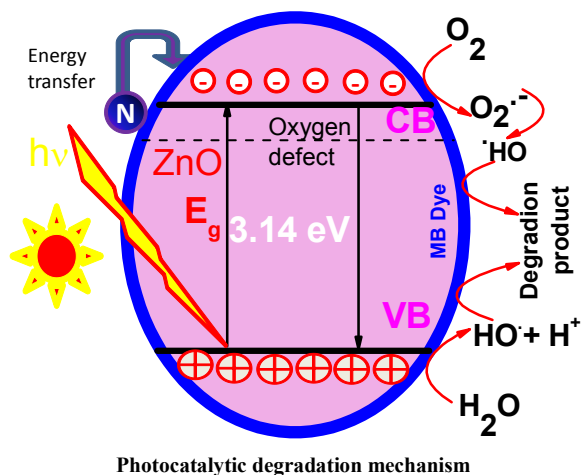


Fig 7 Degradation of MB under dark, visible halogen lamp and solar irradiation.

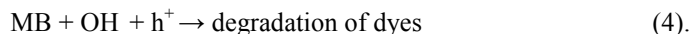
the possible reactions that can occur in photocatalysis process. When the zinc oxide is excited under light irradiation with greater energy than its band gap energy, it will result in the creation of the hole-electron pairs. The hole oxidizes water to produce hydroxyl radicals which are powerful oxidizing agents that efficiently attack organic molecules. The reactions may occur as follows [24, 25].



Formation of OH and O₂⁻ radicals by photogenerated holes and proton respectively,



Degradation of dye via successive attacks by OH radicals and photoholes



CONCLUSION

The formation of N-rich ZnO Nps was studied through the use of Schiff base ligandas a multifunctional agent (nitrogen source, structure directing and capping agent) bythe thermal decomposition method. The nitrogen rich nature of zinc oxide nanostructure was examined by FTIR and EDAX analysis. The optical absorption and band gap was measured using UV-VIS spectrophotometer, which confirmed the semiconducting nature of N-ZnO Nps. The crystal structure (hexagonal) and average crystallite size (52 nm) of synthesized N-ZnO was confirmed by X-ray diffractometer. Pore volume and surface area of the porous N-ZnO was examined by BET analysis. The size of the nanospheres was approximately in the range of 260-300 nm. Microbiology assay finds that N-ZnO nanoparticles are effective against E.coli and K. pneumoniae bacteria. Bacterial analysis reveals that it plays a major role while reacting with antimicrobial agents. Porous N-ZnO nanoparticles showed better photocatalytic activity against methylene blue in visible light irradiation.

Acknowledgement

We thank University of Madras for allowing us to utilize the instrumentation facility.

Reference

1. A. Houas, H. Lachheb, M. Ksibi, E. Elaloui, C. Guillard, J.M. Herrmann, Appl. Catal. B: Environ., 31 (2001) 145-157.
2. E. Lee, A. Benayad, T. Shin, H. Lee, D.S. Ko, T.S. Kim, K.S. Son, M. Ryu, S. Jeon, G.S. Park, Nature Sci. Rep., 4 (2014) 4948-4954.
3. N. Kamarulzaman, M.F. Kasim, and R. Rusdi, Nanoscale Res Lett., 10 (2015) 346-358.
4. C. Klingshirn, C. Phys. Status Solidi B, 71(1975) 547-556.
5. R. Manigandan, K. Giribabu, R. Suresh, L. Vijayalakshmi, A. Stephen, V. Narayanan, Mater. Res. Bull., 48 (2013) 4210-4215.
6. S. Sakthivel, B. Neppolian, M.V. Shankar, B. Arabindoo, M. Palanichamy, V.Murugesan, Sol. Energy Mater. Sol. C, 77 (2003) 65-82.
7. R. Manigandan, K. Giribabu, S. Munusamy, S. Praveen Kumar, S. Muthamizh, T. Dhanasekaran, A. Padmanaban, R. Suresh, A. Stephen, V. Narayanan, CrystEngComm, 17 (2015)2886-2895.
8. J. Zhang, X. Liu, L. Wang, T. Yang, X. Guo, S. Wu, S. Wang and S. Zhang, Nanotechnology, 22 (2011) 185501.
9. W. Wu, S. Zhang, X. Xiao, J. Zhou, F. Ren, L. Sun and C. Jiang, ACS Appl. Mater. Interfaces, 4 (2012) 3602-3609.
10. J. Wang, H. Zhou, J. Zhuang and Q. Liu, Sci. Rep., 3 (2013) 3252-3259.
11. M.K. Debanath, S. Karmakar, Mater. Lett., 111 (2013) 116-119.
12. Y.H. Wang, S.J. Seo, B.S. Bae, J. Mater. Res., 25 (2010) 695-700.

13. G. Nagaraju, S. Ashoka, P. Chithaiah, C.N. Tharamani, G.T. Chandrappa, *Mater. Sci. Semicond. Proc.*, 13 (2010) 21-28.
14. A Guha, J Adhikary, TK Mondal, D Das, *Ind. J. Chem. A*, 50 (2011) 1463-1468.
15. A. García-Raso, J.J. Fiol, A. López-Zafra, I. Mata, E. Espinosa, E. Molins, *Polyhedron*, 19 (2000) 673-680.
16. M.S. Nair, D. Arish, R. S. Joseyphus, *J. Saudi Chem. Soc.*, 16 (2012) 83-88.
17. A.N. Kadam, R.S. Dhabbe, M.R. Kokate, Y.B. Gaikwad, K.M. Garadkar, *Spectrochim. Acta A Mol. Biomol. Spectrosc.*, 133 (2014) 669-676
18. J. C. Wang, Y. Masui and M. Onaka, *Polym. Chem.*, 3 (2012) 865-867.
19. A.A. Soliman and W. Linert, *Thermochim. Acta*, 333 (1999) 67-75
20. G.-P. Hao, W.-C. Li, D. Qian, G.-H. Wang, W.-P. Zhang, T. Zhang, A.-Q. Wang, F. Schueth, H.-J. Bongard and A.-H. Lu, *J. Am. Chem. Soc.*, 133 (2011) 11378-11388.
21. G.-P. Hao, W.-C. Li, D. Qian and A.-H. Lu, *Adv. Mater.*, 22 (2010) 853.
22. A. Laybourn, R. Dawson, R. Clows, J. Iggo, A. Cooper, Y. Khimiyak, D. Adams, *Polym. Chem.*, 3 (2012) 533-537.
23. F. Xu, P. Zhang, A. Navrotsky, Z. Y. Yuan, T.Z. Ren, M. Halasa, and B.L Su, *Chem. Mater.*, 19 (2007) 5680-5686.
24. S. Liu, C. Li, J. Yu and Q. Xiang, *Cryst Eng Comm*, 13 (2011) 2533-2541.
25. X. Liu, H. Du and X.W. Sun, *RSC Adv.*, 4(2014) 5136-5140.

How to cite this article:

Remya Simon et al.2017, Facile Synthesis OF N-ZnO Nanostructures By Thermal Decomposition of Schiff Base Zinc Complex Precursor: Structural, Optical, Antimicrobial And Photocatalytic Properties. *Int J Recent Sci Res.* 8(6), pp. 17640-17645.
DOI: <http://dx.doi.org/10.24327/ijrsr.2017.0806.0396>
